

Modeling of Particle Debonding and Void Evolution in Particulated Ductile Composites

B.R. Kim¹ and H.K. Lee^{1,2}

Abstract: Damage characteristic of particulated ductile composites is a complex evolutionary phenomenon that includes particle debonding and void evolution with the accumulation of the plastic straining of the ductile matrix. In this paper, a micromechanical elastoplastic damage model for ductile matrix composites considering gradually incremental damage (particle debonding and void evolution) is proposed to predict the overall elastoplastic behavior and damage evolution in the composites. The constitutive damage model proposed in an earlier work by the authors [Kim and Lee (2009)] considering particle debonding is extended to accommodate the gradually incremental damage and elastoplastic behavior of the composites. On the basis of the ensemble-averaged effective yield criterion, a micromechanical framework for predicting the effective elastoplastic damage behavior of ductile composites is derived in the present study. A series of numerical simulations including parametric tests are carried out to illustrate stress-strain response of the proposed micromechanical framework. Furthermore, comparisons between the present predictions and experimental data available in the literature are also made to illustrate and assess the predictive capability of the proposed model.

Keywords: Gradually incremental damage, Particle debonding, Void evolution, Elastoplastic damage behavior, Particulated ductile composites

1 Introduction

Particulated ductile composites consist of particles dispersed in a ductile matrix, and the applied load in the composites is shared by the particles and the matrix [Markgraaff (1996)]. Due to the variety of matrices and dispersed inclusions, particulated ductile composites can be manufactured to satisfy a wide range of material properties such as the elastic modulus, strength, and tensile properties.

¹ Department of Civil and Environmental Engineering, Korea Advanced Institute of Science and Technology, Daejeon 305-701, South Korea

² Corresponding author: leeh@kaist.ac.kr

However, due to their heterogeneous characteristics, particulated ductile composites include phases having different material properties, interfaces between the phases, and defects (e.g., microcracks, voids). As a result, these composites have complicated damage mechanisms such as debonding of the matrix-particle interface, brittle fracture of the reinforcing particles, and ductile failuring of the matrix [Drabek and Böhm (2005)]. Although an extensive series of experiments are required in applications of particulated ductile composites, it is time-consuming and difficult to elucidate their mechanical behavior thoroughly due to the aforementioned complex mechanisms [Hussain and Adams (2004); Zong, Zhang, Wang, and Zuo (2007)]. Therefore, the development of a constitutive model that considers both elastoplastic stress-strain relationships as well as the effect of dominant damage mechanisms is essential for an accurate prediction of the behavior of particulated ductile composites.

Various micromechanical approaches have been developed for estimation of mechanical behavior of particulated ductile composites. These approaches can be classified as 1) the effective field approximation (e.g., Eshelby's inclusion method, Mori-Tanaka method, self-consistent method, differential scheme) and 2) discrete microgeometries approximation such as unit cell based model [Aboudi (1989); Böhm and Han (2001); Böhm, Han, and Eckschlager (2004); Li and Wongsto (2004); Pahr and Böhm (2008)], embedding approach [Dong and Schmauder (1996)], windowing methods [Hazanov and Huet (1994); Khisaeva and Ostoja-Starzewski (2006)], and other approaches based on finite element method [Takashima, Nakagaki, and Miyazaki (2007); Haasemann, Kästner, and Ulbricht (2009)]. The details of these micromechanical approaches can be found in Böhm (1998).

Recently, in a preceding work [Kim and Lee (2009)], the authors of this study proposed a damage model that incorporated a cumulative step-stress concept [ReliaSoft (2003)] into the Weibull statistical function for a more realistic simulation of evolutionary particle debonding in composites. The Weibull damage approach has been used for predictions of the interfacial failure or damage in composites.

Zhao and Weng (1995) and Ju and Lee (2000, 2001) proposed a damage model based on the Weibull statistical function to describe the evolutionary interfacial debonding in particle or fiber-reinforced composites. The internal stress of inclusion, denoted by $\bar{\sigma}_p$, was chosen to be the controlling factor of the function, which was required to initiate particle debonding. For simplicity, $\bar{\sigma}_p$ was assumed to be the internal stress of (original) perfectly bonded inclusions. However, in microscale particle debonding, subsequent damage states can be affected by current and previous damage states. Additionally, these damage states accumulate [ReliaSoft (2003); Kim and Lee (2009)]. The cumulative interfacial damage model is recapitulated in Appendix I; the details can be also found in Kim and Lee (2009).

With the accumulation of the plastic straining of the ductile matrix, the voids nucleated by the cumulative interfacial damage between particles and the matrix may grow. The void evolution including void nucleation and growth is the dominant damage factor for predicting the elastoplastic behavior of particulated ductile composites [Huber, Brechet, and Pardoën (2005); Bonfoh and Lipinski (2007)]. Numerous studies of the void evolution in composite materials have been done by many researchers [McClintock (1968); Rice and Tracey (1969); Brown and Embury (1973); Gurson (1977); Tvergaard (1996); Agarwal, Gokhale, Graham, and Horstemeyer (2003); Huber, Brechet, and Pardoën (2005); Bonfoh and Lipinski (2007)].

The present study aims to extend the micromechanical framework of our preceding work [Kim and Lee (2009)] to accommodate the overall elastoplastic behavior of particulated ductile composites together with the gradually incremental damage considering cumulative particle debonding and void evolution. The influence of the gradually incremental damage on the elastic and elastoplastic responses of the composites is also investigated. Micromechanical formulations combining the effective elastic moduli of composites proposed by the authors [Kim and Lee (2009)] and the elastoplastic formulation of the ductile matrix under arbitrary three-dimensional (3D) loading/unloading histories are proposed to predict the effective elastoplastic behavior of particulated ductile composites. All particles in particulated ductile composites are assumed to be randomly dispersed elastic spheres that are non-interacting and initially bonded perfectly in a ductile matrix.

As loads or deformations increase, some perfectly bonded particles are assumed to lose their load-carrying capacity along the debonded direction and become partially debonded particles in the initial (first) damage state. It is assumed that some partially debonded particles are regarded as equivalent, transversely isotropic inclusions after particle debonding between particles and the ductile matrix [Ju and Lee (2001)]. Furthermore, as loads or deformations further increase, some partially debonded particles are assumed to lose all of their load-carrying capacity and finally become completely debonded. It is also assumed that the completely debonded particles are replaced by the voids having the same volume fraction (see also, Bonfoh and Lipinski (2007)). By Kim and Lee (2009), a comparison between noncumulative and cumulative damage models was carried out to investigate the influence of the cumulative (interfacial debonding) damage on the interfacial damage evolution in composites. Here, the values of the internal stress of the particles $\bar{\sigma}_p$ and the Weibull parameter S_0 are changed as the damage state evolves in both damage models.

The present study focuses on the gradually incremental damage behavior and elastoplastic behavior of particulated ductile composites. A series of numerical simula-

tions including parametric tests are carried out to illustrate stress-strain response of the proposed micromechanical framework. Furthermore, comparisons between the present predictions and experimental data available in the literature are made to illustrate and assess the predictive capability of the proposed model.

2 Effective elastoplastic behavior of particulated ductile composites

Several studies to characterize the damage in particulated ductile composites have proposed the use of the Weibull statistics for damage evolution. Studies for assessing the vulnerability of reinforcing particles to brittle fracturing have been conducted by Wallin, Saario, and Törrönen (1987), Lewis and Withers (1995), Antretter and Fischer (1998), Ghosh and Moorthy (1998), LLorca and González (1998) and Han, Eckschlager, and Böhm (2001). However, due to the superior material properties of particles compared with the matrix, the damage in the matrix and the interface between particles and the matrix rather than the damage of the particles has to be treated preferentially for the characterization of the mechanical behavior of particulated ductile composites [Inem and Pollard (1993); Tohgo and Weng (1994); Rajan, Pillai, and Pai (1998); Evans (1999); Chen, Huang, and Mai (2003); Liu, Sun, and Ju (2004)]. From this viewpoint, this study focuses on the ductile damage such as particle debonding and void evolution in particulated ductile composites. In particular, a cumulative interfacial damage model and a void evolution model are employed for a more realistic simulation of gradually incremental damage in particulated ductile composites.

For the formulation of the elastoplastic damage response of particulated ductile composites, let us consider an initially perfectly bonded two-phase composite consisting of an elastoplastic matrix (phase 0) with an elastic bulk modulus κ_0 and an elastic shear modulus μ_0 , and perfectly bonded elastic spherical particles (phase 1) with a bulk modulus κ_1 and an elastic shear modulus μ_1 subjected to a uniaxial tensile loading. As loads or deformations increase, evolutionary damage between particles and the matrix in the composite may occur.

In the present derivation, it is assumed that the composite undergoes a two-step damage process as follows: some perfectly bonded particles lose their load-carrying capacity along the debonded direction and become partially debonded particles (phase 2) in the initial (first) damage state and some partially debonded particles lose their total load-carrying capacity and finally become completely debonded particles in the final damage state as loads or deformations continue to increase [Kim and Lee (2009)]. Here, the completely debonded particles are regarded as voids (phase 3) having the same volume fraction. A schematic description of the gradually incremental damage in particulated ductile composites subjected to a uniaxial tension is shown in Fig. 1.

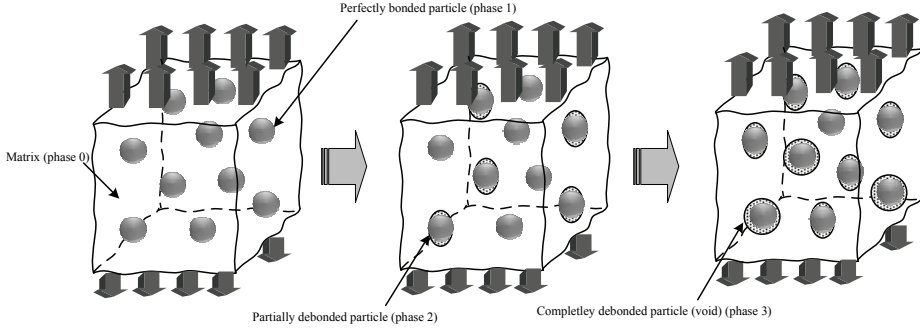


Figure 1: A schematic description of the gradually incremental damage in particulated ductile composites subjected to a uniaxial tension

The cumulative damage model proposed by Kim and Lee (2009) recapitulated in Appendix I is employed here to model the particle debonding. The volume fraction of the r -phase inclusion according to the cumulative particle debonding between perfectly bonded or partially debonded particles and the matrix are also formulated in Appendix I. The volume fraction of voids (the completely debonded particles) initially nucleated by particle debonding is assumed to increase as the voids grow. Since the volume fraction of voids is governed by void nucleation and void growth rates, the incremental form of volume fraction of voids can be expressed as [cf., Bonhof and Lipinski (2007)]

$$\Delta\phi_3 = \Delta\phi_3^n + \Delta\phi_3^g \quad (1)$$

where $\Delta\phi_3^n$ and $\Delta\phi_3^g$ denote the incremental form of volume fraction of voids due to their nucleation and growth, respectively. Following Eq. (21) in Appendix I, $\Delta\phi_3^n$ reads

$$\Delta\phi_3^n = (\phi_3)_{i+1} - (\phi_3)_i \quad (2)$$

in which the subscript i denotes the iteration number of stress increment. In addition, $\Delta\phi_3^g$ can be expressed as [cf., Bonhof and Lipinski (2007)]

$$\Delta\phi_3^g = (1 - \phi)\Delta\varepsilon_{ii}^p \quad (3)$$

where ϕ is the (original) volume fraction of the particles and ε_{ii}^p denotes the ii components of the overall plastic strain.

The elastic strain $\bar{\boldsymbol{\varepsilon}}^e$ of the composite can be directly obtained by using the following constitutive relation between the macroscopic stress $\bar{\boldsymbol{\sigma}}$ and the elastic strain

$\bar{\boldsymbol{\epsilon}}^e$:

$$\bar{\boldsymbol{\sigma}} = \mathbf{C}_* : \bar{\boldsymbol{\epsilon}}^e \tag{4}$$

where the effective stiffness of the four-phase composite \mathbf{C}_* was explicitly derived by Kim and Lee (2009) as

$$\mathbf{C}_* = \tilde{\mathbf{F}}_{ijkl}(c_1, c_2, c_3, c_4, c_5, c_6) \tag{5}$$

in which the parameters c_1, \dots, c_6 can be found in Eqs. (19)-(24) of Kim and Lee (2009) and details of the transversely isotropic fourth-rank tensor $\tilde{\mathbf{F}}$ can be found in Ju and Lee (2001).

For the elastoplastic behavior of the ductile matrix of particulated ductile composites, the J_2 -type von-Mises yield criterion with isotropic hardening law is adopted. Accordingly, the following yield criterion is valid [see, e.g., Ju and Tseng (1996); Ju and Lee (2000); Lee and Pyo (2008)].

$$F(\boldsymbol{\sigma}, \bar{\epsilon}^p) = H(\boldsymbol{\sigma}) - K^2(\bar{\epsilon}^p) \leq 0 \tag{6}$$

where $\boldsymbol{\sigma}$ and $\bar{\epsilon}^p$ are the stress and the equivalent plastic strain at any point in the matrix, respectively. In addition, $K(\bar{\epsilon}^p)$ signifies the isotropic hardening function of the matrix and $H(\boldsymbol{\sigma}) \equiv \boldsymbol{\sigma} : \mathbf{I}_d : \boldsymbol{\sigma}$ is the square of the deviatoric stress norm in which \mathbf{I}_d denotes the deviatoric part of the fourth-rank identity tensor \mathbf{I} [Ju and Lee (2000)].

The ensemble average of $H(\mathbf{x}|\bar{\boldsymbol{\omega}})$ over all possible realizations in which \mathbf{x} is in the ductile matrix, denoted by $H(\mathbf{x}|\bar{\boldsymbol{\omega}}) = \boldsymbol{\sigma}(\mathbf{x}|\bar{\boldsymbol{\omega}}) : \mathbf{I}_d : \boldsymbol{\sigma}(\mathbf{x}|\bar{\boldsymbol{\omega}})$ [Ju and Chen (1994); Ju and Tseng (1996); Ju and Lee (2000, 2001); Ju and Sun (2001); Lee and Pyo (2008)], can be evaluated by collecting and summing up all the current stress norm perturbations produced by any inclusions centered at $\mathbf{x}_q^{(1)}$ ($q=1-3$) in q -phase inclusions and averaging over all possible locations of $\mathbf{x}_q^{(1)}$. Accordingly, the ensemble average of $H(\mathbf{x}|\bar{\boldsymbol{\omega}})$ can be recast into a more simplified form [cf., Ju and Lee (2000, 2001)]:

$$\begin{aligned} \langle H \rangle_m(\mathbf{x}) \cong & H^0 + \frac{N_1}{V} \int_{\hat{r}_1} d\hat{r}_1 \int_{A(\hat{r}_1)} \{H(\hat{\mathbf{r}}_1) - H^0\} dA + \\ & \frac{N_2}{V} \int_{\hat{r}_2} d\hat{r}_2 \int_{A(\hat{r}_2)} \{H(\hat{\mathbf{r}}_2) - H^0\} dA + \frac{N_3}{V} \int_{\hat{r}_3} d\hat{r}_3 \int_{A(\hat{r}_3)} \{H(\hat{\mathbf{r}}_3) - H^0\} dA + \dots \end{aligned} \tag{7}$$

Here, $H^0 = \boldsymbol{\sigma}^0 : \mathbf{I}_d : \boldsymbol{\sigma}^0$, where $\boldsymbol{\sigma}^0$ is the far-field stress, is the square of the far-field stress norm in the matrix, and N_q is the total numbers of q -phase inclusions

dispersed in a representative volume V . In addition, $A(\hat{r}_q)$ is a spherical surface of radius \hat{r}_q ($q=1-3$) with $\hat{\mathbf{r}}_q = \mathbf{x} - \mathbf{x}_q$ and $\hat{r}_q \equiv \|\hat{\mathbf{r}}_q\|$.

By using the two identities in Ju and Chen (1994) and the five identity groups and inner product of the fourth-rank tensor in Ju and Lee (2001), the ensemble-averaged current stress norm at any point in the matrix can be derived after a series of lengthy derivations as

$$\langle H \rangle_m(\mathbf{x}) = \boldsymbol{\sigma}^0 : \mathbf{T} : \boldsymbol{\sigma}^0 = \bar{\boldsymbol{\sigma}} : \bar{\mathbf{T}} : \bar{\boldsymbol{\sigma}} \quad (8)$$

where $\boldsymbol{\sigma}^0$ and $\bar{\boldsymbol{\sigma}}$ signify the far-field stress and the macroscopic stress, respectively. From the relation between $\boldsymbol{\sigma}^0$ and $\bar{\boldsymbol{\sigma}}$ expressed as $\boldsymbol{\sigma}^0 = \mathbf{P} : \bar{\boldsymbol{\sigma}}$ [Ju and Lee (2000, 2001)], the relation between the positive definite fourth-rank tensors \mathbf{T} and $\bar{\mathbf{T}}$ is defined as

$$\bar{\mathbf{T}} \equiv \mathbf{P}^T \cdot \mathbf{T} \cdot \mathbf{P} \quad (9)$$

in which the components of the positive definite fourth-rank tensor \mathbf{T} , \mathbf{P} , and $\bar{\mathbf{T}}$ read

$$T_{ijkl} = T_1 \tilde{n}_i \tilde{n}_j \tilde{n}_k \tilde{n}_l + T_2 (\delta_{ik} \tilde{n}_j \tilde{n}_l + \delta_{il} \tilde{n}_j \tilde{n}_k + \delta_{jk} \tilde{n}_i \tilde{n}_l + \delta_{jl} \tilde{n}_i \tilde{n}_k) + T_3 \delta_{ij} \tilde{n}_k \tilde{n}_l + T_4 \delta_{kl} \tilde{n}_i \tilde{n}_j + T_5 \delta_{ij} \delta_{kl} + T_6 (\delta_{ik} \delta_{jl} + \delta_{il} \delta_{jk}) \quad (10)$$

$$P_{ijkl} = P_1 \tilde{n}_i \tilde{n}_j \tilde{n}_k \tilde{n}_l + P_2 (\delta_{ik} \tilde{n}_j \tilde{n}_l + \delta_{il} \tilde{n}_j \tilde{n}_k + \delta_{jk} \tilde{n}_i \tilde{n}_l + \delta_{jl} \tilde{n}_i \tilde{n}_k) + P_3 \delta_{ij} \tilde{n}_k \tilde{n}_l + P_4 \delta_{kl} \tilde{n}_i \tilde{n}_j + P_5 \delta_{ij} \delta_{kl} + P_6 (\delta_{ik} \delta_{jl} + \delta_{il} \delta_{jk}) \quad (11)$$

$$\bar{T}_{ijkl} = \bar{T}_1 \tilde{n}_i \tilde{n}_j \tilde{n}_k \tilde{n}_l + \bar{T}_2 (\delta_{ik} \tilde{n}_j \tilde{n}_l + \delta_{il} \tilde{n}_j \tilde{n}_k + \delta_{jk} \tilde{n}_i \tilde{n}_l + \delta_{jl} \tilde{n}_i \tilde{n}_k) + \bar{T}_3 \delta_{ij} \tilde{n}_k \tilde{n}_l + \bar{T}_4 \delta_{kl} \tilde{n}_i \tilde{n}_j + \bar{T}_5 \delta_{ij} \delta_{kl} + \bar{T}_6 (\delta_{ik} \delta_{jl} + \delta_{il} \delta_{jk}) \quad (12)$$

in which the parameters T_1, \dots, T_6 for fourth-rank tensor \mathbf{T} and the parameters P_1, \dots, P_6 for fourth-rank tensor \mathbf{P} are given in Appendices II and III, respectively. The components of the fourth-rank tensor $\bar{\mathbf{T}}$ can be derived by replacing (P_1^p, \dots, P_6^p) and (T_1^p, \dots, T_6^p) in Eqs. (61)-(66) of Ju and Lee (2001) with (P_1, \dots, P_6) and (T_1, \dots, T_6) in Appendices III and II, respectively.

According to Ju and Lee (2000, 2001), the ensemble-averaged current stress norm for any point \mathbf{x} in the four-phase composite can be defined as

$$\sqrt{\langle H \rangle(\mathbf{x})} = (1 - \phi_1) \sqrt{\bar{\boldsymbol{\sigma}} : \bar{\mathbf{T}} : \bar{\boldsymbol{\sigma}}} \quad (13)$$

where ϕ_1 is the volume fraction of current perfectly bonded fibers. Accordingly, the effective yield function for the four-phase composite given in Eq.(6) becomes

$$\bar{F} = (1 - \phi_1)^2 \bar{\boldsymbol{\sigma}} : \bar{\mathbf{T}} : \bar{\boldsymbol{\sigma}} - K^2 (\bar{e}^p) \quad (14)$$

In addition, the following simple power-law type isotropic hardening function is adopted here.

$$K(\bar{\epsilon}^p) = \sqrt{\frac{2}{3}} \{ \sigma_y + h(\bar{\epsilon}^p)^q \} \quad (15)$$

where σ_y denotes the initial yield stress, and h and q signify the linear and exponential isotropic hardening parameters, respectively [see also, Ju and Lee (2000, 2001)]. The effective ensemble-averaged plastic strain rate $\dot{\bar{\epsilon}}^p$ and the effective equivalent plastic strain rate $\dot{\bar{\epsilon}}^p$ required for obtaining the ensemble-averaged current stress norm are defined in Eqs. (69) and (70) of Ju and Lee (2001), respectively. Details of the elastoplastic stress-strain relation under uniaxial tension can also be found in Ju and Lee (2001) and Lee and Simunovic (2001).

3 Predictions of elastoplastic damage response of particulated ductile composites

To illustrate the proposed micromechanical framework, the elastoplastic response of SiC particulate reinforced Al-Cu matrix composites (20% in particle volume fractions) is predicted using the proposed model. The constituent properties and plastic parameters of the composites are adopted from those used in Ju and Lee (2000) as follows: $E_m=55.8$ GPa, $\nu_m=0.32$, $E_p=397$ GPa, $\nu_p=0.2$; $\sigma_y=87.8$ MPa, $h=972$ MPa, $q=0.55$, where the subscripts m and p denote the matrix and particles, respectively. The predicted stress-strain response of the particulated ductile composites is shown in Fig. 2 and can be divided into four parts as:

- (a) The linear part OA in the stress-strain curve reflects the elastic behavior of particulated ductile composites where no significant damage occurs.
- (b) The AB part illustrates a nonlinear behavior of the composites caused by particle interfacial debonding as shown in the evolution curve for partially debonded particles in the figure.
- (c) The BC part in the stress-strain curve, distinguished from the AB part, indicate that the void growth initiated at the starting point of plastic behavior (point B) and the void nucleation by particle interfacial debonding have an influence on the nonlinear behavior of the composites.
- (d) The CD part in the stress-strain curve corresponds to the plastic behavior following the isotropic hardening law/flow rule and ductile damage caused by the void evolution.

A series of parametric tests for the gradually incremental damage and elastoplastic behavior of the composites are conducted next. In this simulation, the value of the Weibull parameter $(S_0)_1$ related to the first damage state is fixed to be:

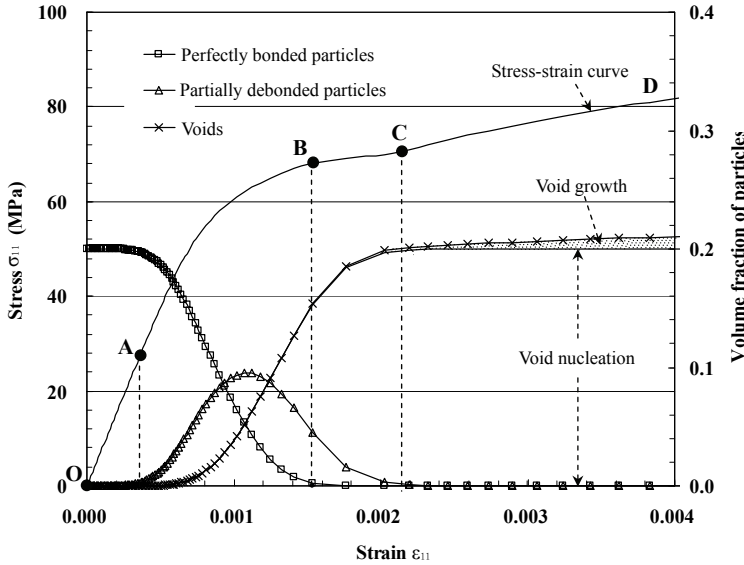
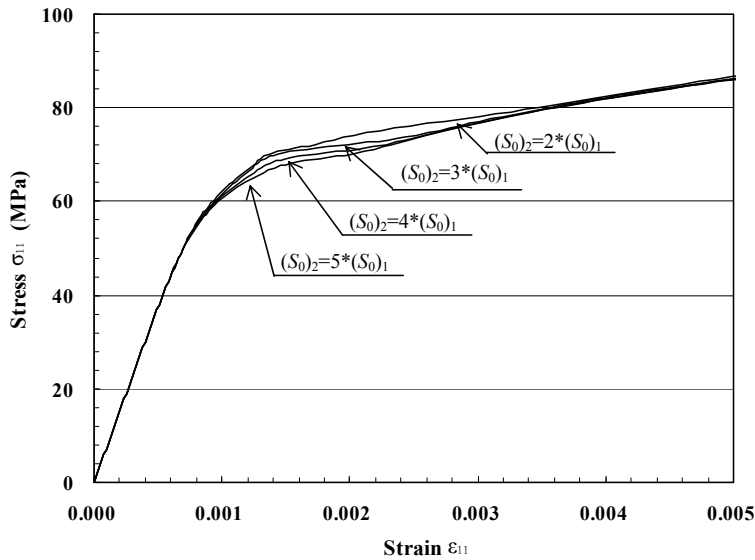
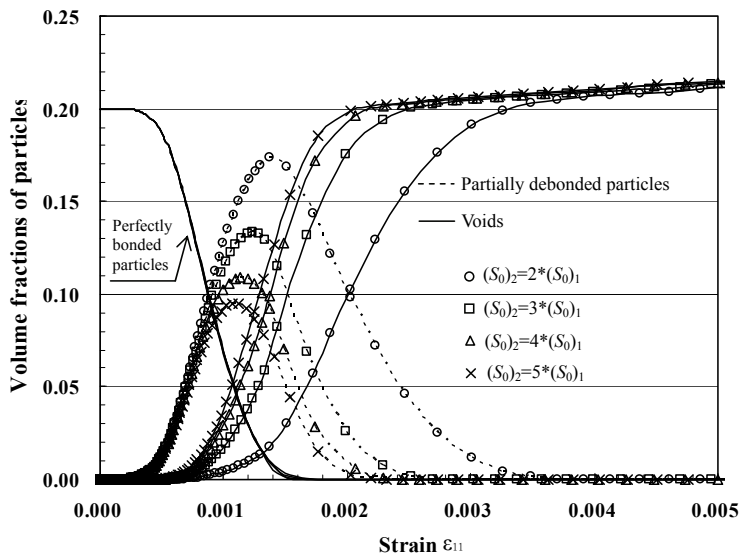


Figure 2: The predicted stress-strain curve of particulated ductile composites

$(S_0)_1 = 1.09 \cdot \sigma_y$, whereas various values of the Weibull parameters $(S_0)_2$ related to the second damage state are considered ($(S_0)_2 = 2 \cdot (S_0)_1, 3 \cdot (S_0)_1, 4 \cdot (S_0)_1, 5 \cdot (S_0)_1$) in order to examine the influence of $(S_0)_2$ on the elastoplastic response of the composites. Fig. 3 shows the predicted stress-strain curves of the composites and the corresponding damage evolution curves. As noted in Kim and Lee (2009), it is shown from Fig. 3(a) that the Weibull parameter $(S_0)_2$ has a significant influence on the damage evolution in particulated ductile composites and partially debonded particles rapidly become completely debonded particles as $(S_0)_2$ value continues to increase. This phenomenon can be clearly observed in the damage evolution curves in Fig. 3(b). Fig. 4 shows the variation of the normalized elastic moduli E/E_0 according to the gradually incremental damage. Here, E_0 and E denote the initial Young's modulus and the current Young's modulus due to the gradually incremental damage in particulated ductile composites, respectively. It is also clear that the gradually incremental damage shown in Fig. 3 results in the degradation of the elastic modulus. Sharp degradation occurs as $(S_0)_2$ value continues to increase. A parametric test on the Weibull parameter M is also carried out. The predicted stress-strain curves and corresponding damage evolution curves are presented in Figs. 5 and 6, respectively. The initiation and termination of the particle debonding for each M value are marked on the stress-strain curves to clearly illustrate the region affected by the particle debonding ("particle debonding region") in Fig. 5.

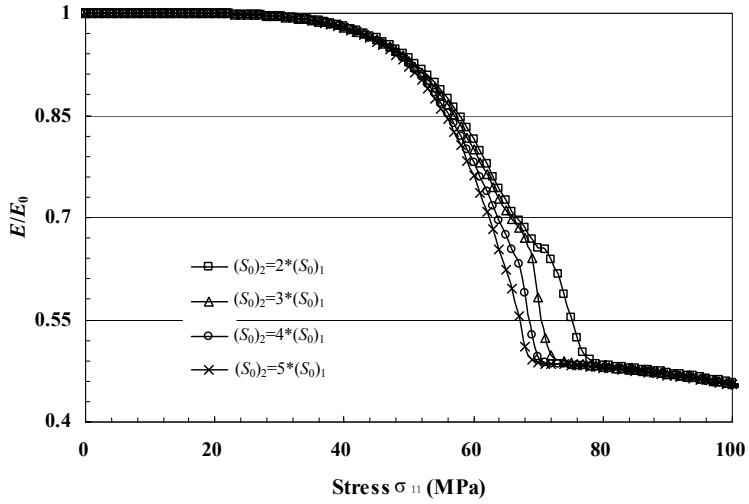


(a)

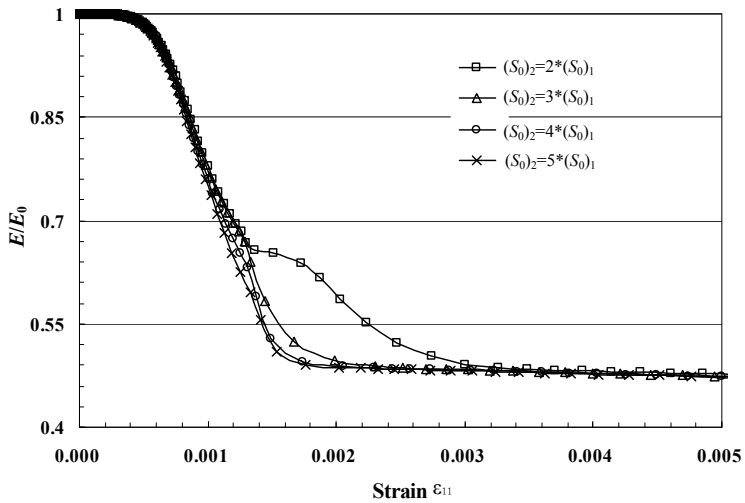


(b)

Figure 3: The stress-strain curves of particulated ductile composites predicted by the proposed gradually incremental damage model (a) and the corresponding damage evolution curves (b)



(a)



(b)

Figure 4: Variation of normalized elastic moduli (E/E_0) according to stress (a) and strain (b)

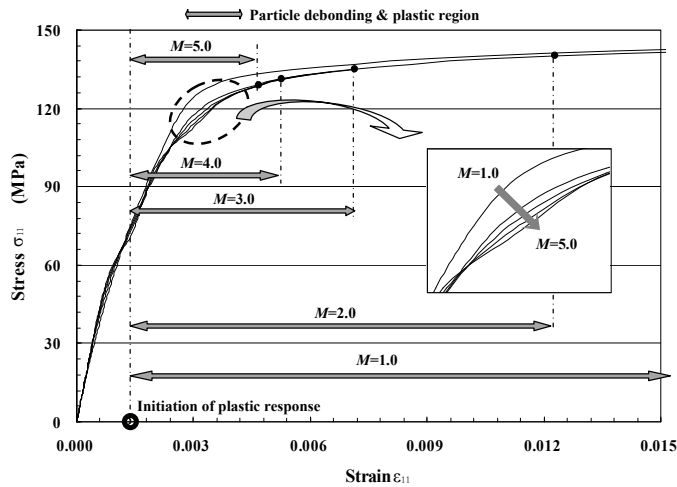


Figure 5: The predicted stress-strain curves of particulated ductile composites with various M values ($(S_0)_1 = 1.09 * \sigma_y$, $(S_0)_2 = 2 * (S_0)_1$, $h = 200 \text{ MPa}$, $q = 0.1$)

It is observed from Figs. 5 and 6 that the particle debonding region grows as the M value decreases.

Another parametric test on the plastic parameters h and q is conducted to identify the influence of those parameters on the elastoplastic behavior of the composites. The predicted stress-strain curves of the composites with various h and q values are exhibited in Fig. 7. It is shown, as expected, that the stress-strain curves increase as h value increases, whereas the stress-strain curves decrease as the q value increases. The influence of the q value on the elastoplastic response is shown to be more pronounced than that of the h value due to the different nature of these parameters.

4 Characteristics of the nonlinear stress-strain response of particulated ductile composites

The characteristics of the nonlinear stress-strain response of particulated ductile composites are thoroughly investigated in this section. A comprehensive understanding of the characteristics of the nonlinear stress-strain response, mainly due to damage and ductility, in particulated ductile composites is essential for an accurate characterization of particulated ductile composites. In this section, the influence of the initiation and termination of particle debonding on the effective elastoplastic behavior of the composites is investigated for a better understanding of the characteristics of the nonlinear stress-strain response of the composites. Only the particle

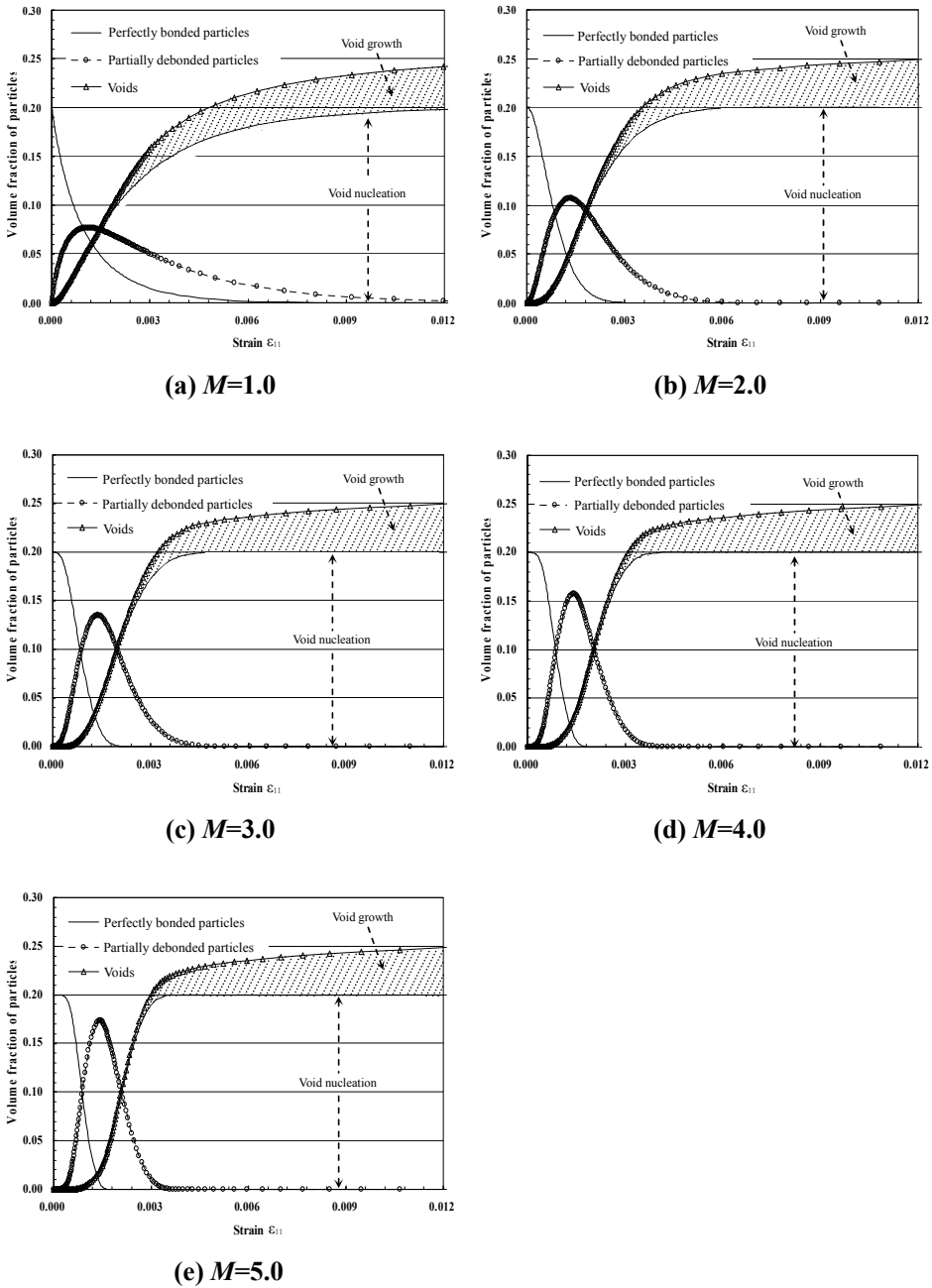


Figure 6: The damage evolution curves corresponding to the predicted stress-strain curves in Fig. 5

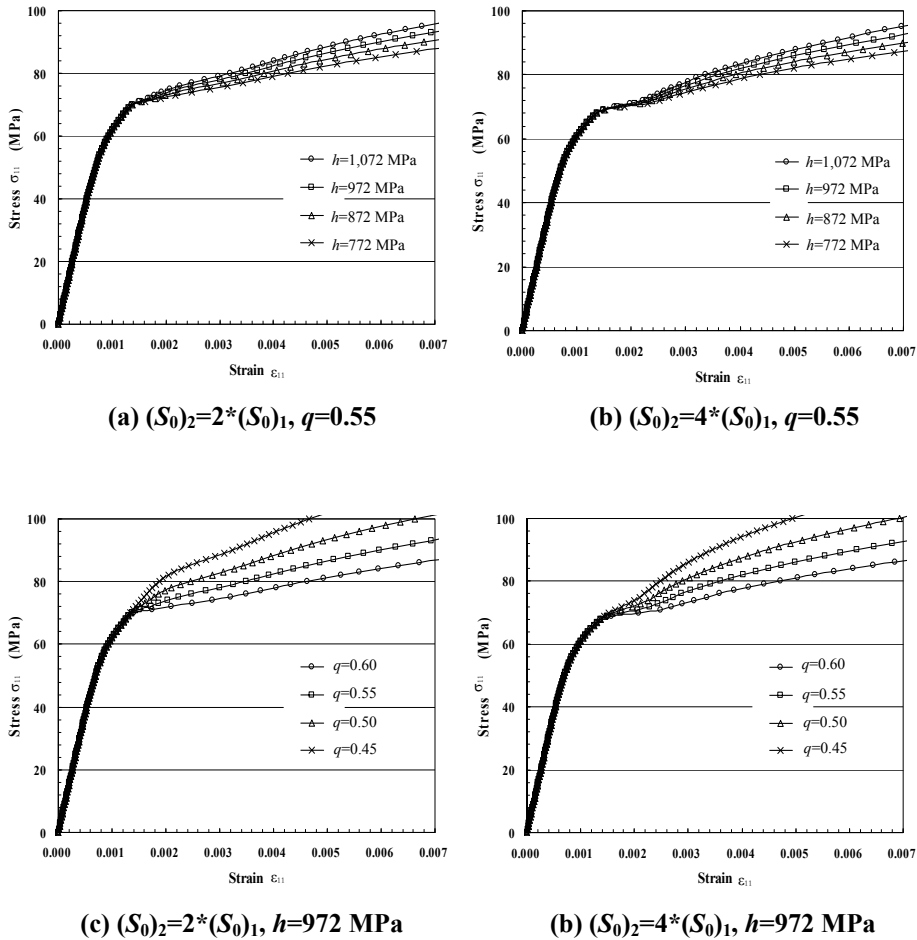


Figure 7: The predicted stress-strain curves of particulated ductile composites with various h and q values

debonding and ductility of the matrix, two dominant factors affecting the nonlinear behavior of the composites, are considered in this simulation. The values of the Weibull parameters $(S_0)_1$ and the plastic parameters h and q are fixed to be: $(S_0)_1=1.09*\sigma_y$, $h=700 \text{ MPa}$, and $q=0.5$, for simplicity. Two different values of the Weibull parameter $(S_0)_2$ related to the second damage state and the Weibull parameter M are used: $(S_0)_2=10*(S_0)_1, M=7$; $(S_0)_2=2*(S_0)_1, M=5$ for a clear representation of the two different nonlinear stress-strain responses of the composites.

A two-step nonlinear stress-strain response, comprising the particle debonding re-

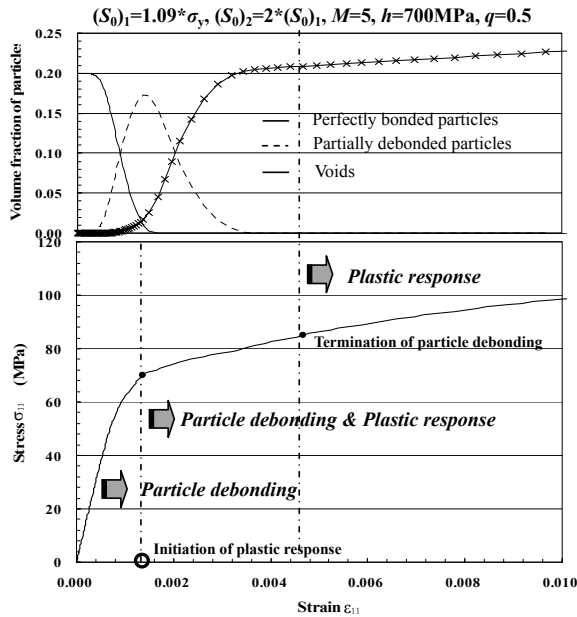
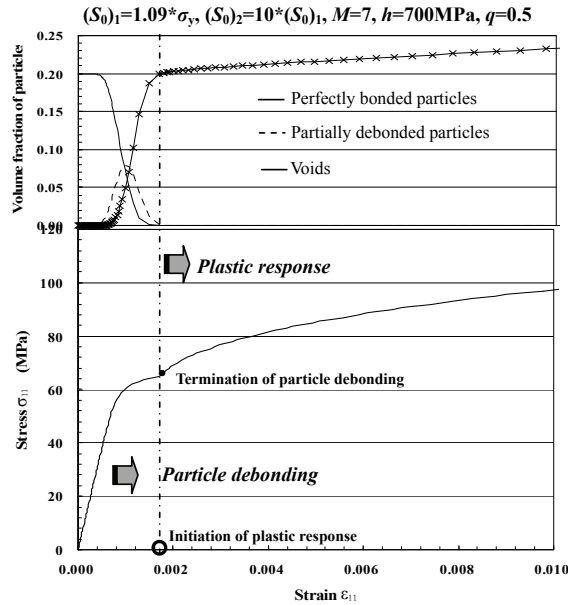
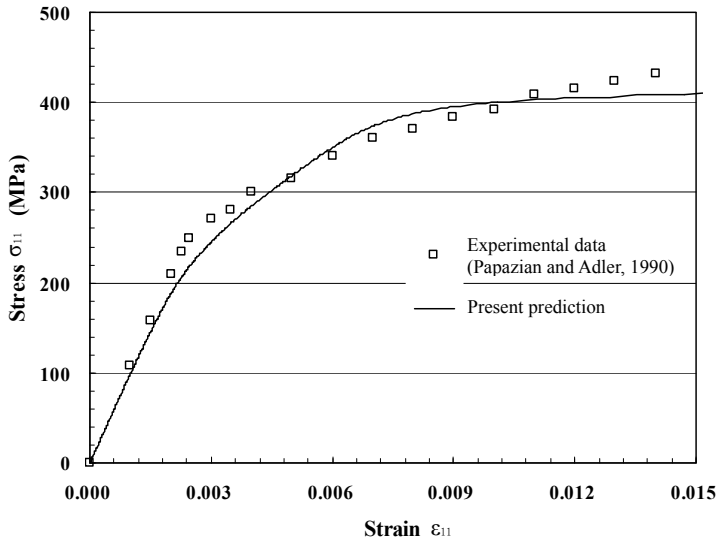
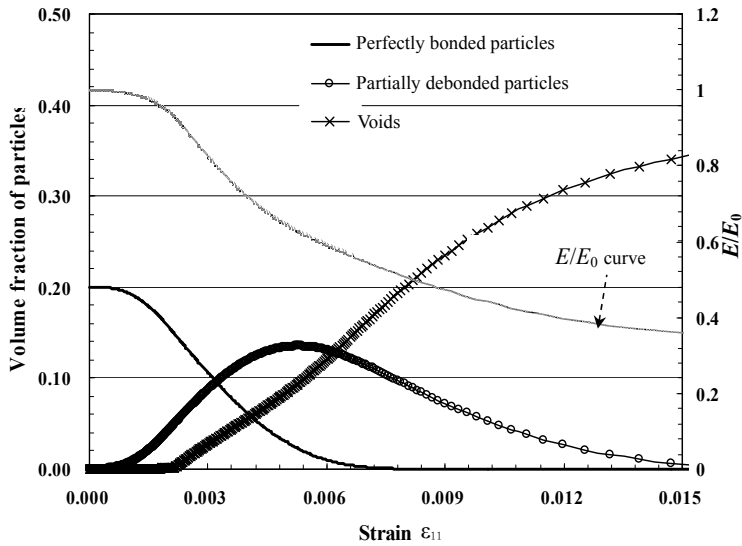


Figure 8: Two different nonlinear stress-strain responses in particulated ductile composites: (a) two-step nonlinear stress-strain response and (b) three-step nonlinear stress-strain response



(a)



(b)

Figure 9: Comparison of stress-strain curves between the present prediction and experimental data [Papazian and Adler (1990)] (a) and damage evolution curves and E/E_0 curve corresponding to the predicted stress-strain curve (b)

gion and the plastic region, along with a three-step nonlinear stress-strain response comprising the particle debonding region, the particle debonding and plastic region, and the plastic region, are observed, as shown in Fig. 8. In both two-step and three-step nonlinear stress-strain response cases, the initial nonlinear stress-strain response is primarily due to the particle debonding between particles and the matrix. When $(S_0)_2=10*(S_0)_1$, the evolution of partially debonded particles into voids accelerates, resulting in a rapid saturation of partially debonded particles into completely debonding particles even prior to the initiation of the plastic response (two-step stress-strain response), as shown in Fig. 8(a).

In contrast, a three-step nonlinear stress-strain response is observed when the value of the Weibull parameter $(S_0)_2$ is low (Fig. 8(b)). It can thus be summarized that accurate characterization of Weibull parameters is desirable for a realistic performance prediction of particulated ductile composites since the Weibull parameter $(S_0)_2$ influences the effective elastoplastic behavior of ductile matrix composites.

5 Experimental comparison

To highlight the applicability of the present model for predicting the elastoplastic incremental damage behavior of particulated ductile composites, the present predictions are compared with experimental data available in the literature [Papazian and Adler (1990); Llorca, Needleman, and Suresh (1991)]. The mechanical behavior of SiC particulate-reinforced aluminum alloy matrix composites under uniaxial tension is predicted and the results are compared with the experimental data reported by Papazian and Adler (1990). The material properties of the composites are adopted according to Papazian and Adler (1990) as follows: $E_m=73$ GPa, $\nu_m=0.33$, and $E_p=485$ GPa, $\nu_p=0.2$, $\phi=20\%$, and $\sigma_y=230$ MPa. As the Weibull parameters and plastic parameters were not reported in Papazian and Adler (1990), these parameters are estimated in accordance with the experimental data reported in Papazian and Adler (1990) as: $h=1072$ MPa, $q=0.11$, $(S_0)_1=445$ MPa, $(S_0)_2=2*(S_0)_1$, and $M=3.0$.

Fig. 9(a) shows a comparison of stress-strain curves between the present predictions using the gradually incremental damage model and the experimental data [Papazian and Adler (1990)]. The stress-strain curves beyond $\epsilon_{11}=0.015$ are not displayed due to the small-strain constraint of the proposed model [Ju and Lee (2000)]. The evolution of the volume fractions of perfectly bonded particles, partially debonded particles, and voids corresponding to the present predictions in Fig. 9(a) are shown in Fig. 9(b). The evolution curve of the normalized elastic moduli is also plotted in Fig. 9(b). Fig. 9(a) shows that the stress-strain curve predicted by the proposed gradually incremental damage model is in good quantitative agreement with the experimental data.

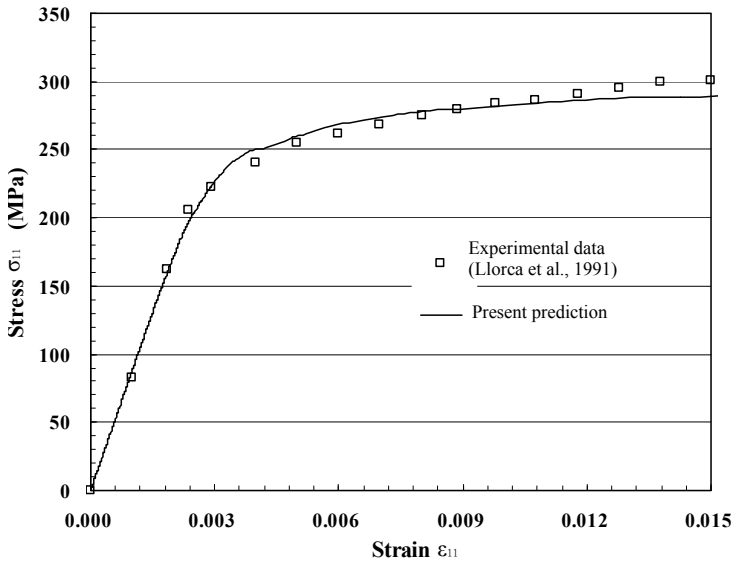
The present prediction is also compared with the experimental data of Llorca, Needleman, and Suresh (1991) to further assess the predictive capability of the proposed model. The uniaxial stress-strain behavior of an Al-Cu matrix containing SiC particles is predicted and the results are compared with the experimental data [Llorca, Needleman, and Suresh (1991)]. The material properties of the composites are adopted in accordance with Llorca, Needleman, and Suresh (1991) as: $E_m=71.8$ GPa, $\nu_m=0.33$, and $E_p=450$ GPa, $\nu_p=0.17$, $\phi=13\%$, and $\sigma_y=170$ MPa. In accordance with the experimental data documented in Llorca, Needleman, and Suresh (1991), the Weibull and plastic parameters are estimated to be: $(S_0)_1=380$ MPa, $(S_0)_2=2*(S_0)_1$, and $M=5.0$ (for particle debonding); $h=512$ MPa and $q=0.15$ (for plastic behavior).

Based on the above Weibull and plastic parameters, the comparison of stress-strain curves between the present predictions and the experimental data [Llorca, Needleman, and Suresh (1991)] is made and the results are shown in Fig. 10(a). The incremental damage evolution curves and evolution curve of the normalized elastic moduli corresponding to the predicted stress-strain curve in Fig. 10(a) are shown in Fig. 10(b). The stress-strain curve in Fig. 10(a) predicted by the gradually incremental damage model is shown to have a good correlation with the experimental data on dilute particulated ductile composites. Good agreements between the present prediction and experimental data verify the predictive capability of the proposed micromechanical elastoplastic model considering the gradually incremental damage.

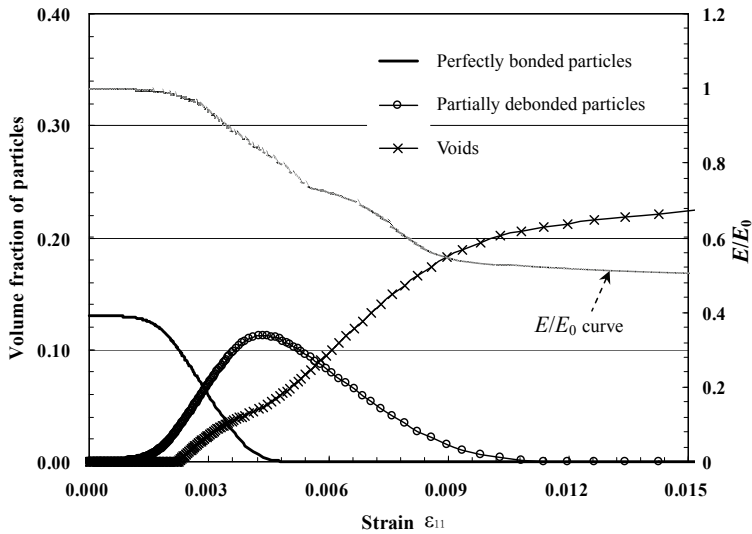
6 Concluding remarks

A micromechanical elastoplastic damage model for ductile matrix composites considering gradually incremental damage (particle debonding and void evolution) has been proposed to predict the overall elastoplastic behavior and damage evolution in the composites. The constitutive damage model [Kim and Lee (2009)] considering particle debonding is extended to accommodate the gradually incremental damage and elastoplastic behavior of the composites. Based on the ensemble-averaged effective yield criterion, a micromechanical framework for predicting the effective elastoplastic damage behavior of ductile composites is derived in the present study. A series of numerical simulations and comparisons between the present predictions and experimental data available in the literature are made to illustrate and assess the predictive capability of the proposed model. The findings of the present study can be summarized as follows:

- 1) As loads or deformations continue to increase, damage induced by particle debonding in composites is accumulated and affects the behavior of composites.



(a)



(b)

Figure 10: Comparison of stress-strain curves between the present prediction and experimental data [Llorca, Needleman, and Suresh (1991)] (a) and damage evolution curves and E/E_0 curve corresponding to the predicted stress-strain curve (b)

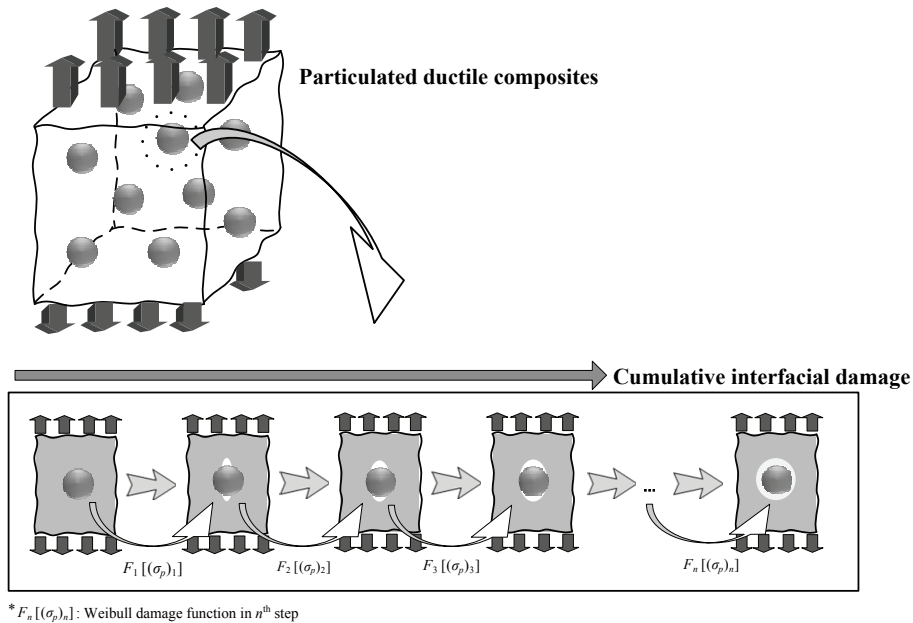


Figure 11: The schematic description of the gradually incremental damage model [cf., Fig. 2 of Kim and Lee (2009)]

- 2) The voids nucleated by the cumulative interfacial damage between particles and the matrix grow with the accumulation of plastic deformation. This phenomenon causes the progressive damage behavior of ductile matrix composites.
- 3) The Weibull damage parameters (e.g., $(S_0)_2$) have a significant influence on the damage evolution in composites, resulting in different nonlinear stress-strain responses.
- 4) Various damage phenomena in ductile matrix composites are simulated using the proposed model by varying values of the Weibull damage parameters and plastic parameters.

The present study has demonstrated the capability of the proposed micromechanical framework for predicting the elastoplastic damage behavior of composites. The proposed micromechanical elastoplastic model is shown to be suitable for the performance prediction of particle-reinforced ductile matrix composites with gradually incremental damage. However, a unified experimental and numerical study should be carried out to calibrate the model parameters of the proposed model.

Acknowledgement: This research was sponsored by the Korea Science and En-

gineering Foundation (KOSEF) grant funded by the Korea government (MEST 20090080587) and the IT R&D program of MKE/KEIT (2008-F-044-02, Development of new IT convergence technology for smart building to improve the environment of electromagnetic waves, sound and building).

References

- Aboudi, J.** (1989): Micromechanical analysis of composites by the method of cells. *Applied Mechanics Reviews*, vol. 42, pp. 193-221.
- Agarwal, H.; Gokhale, A.M.; Graham, S.; Horstemeyer, M.F.** (2003): Void growth in 6061-aluminum alloy under triaxial stress state. *Materials Science and Engineering*, vol. A341, pp. 35-42.
- Antretter, T.; Fischer, F.D.** (1998): Particle cleavage and ductile crack growth in a two-phase composite on a microscale. *Computational Materials Science*, vol. 13, pp. 1-7.
- Ashby, M.F.** (1989): On the engineering properties of materials. *Acta Metallurgica*, vol. 37, no. 5, pp. 1273-1293.
- Böhm, H.J.** (1998): *A short introduction to basic aspects of continuum micromechanics*, CDL-FMD Report 3-1998, TU Wien, Vienna.
- Böhm, H.J.; Han, W.** (2001): Comparisons between three-dimensional and two-dimensional multi-particle unit cell models for particle reinforced MMCs. *Modelling and Simulation in Materials Science and Engineering*, vol. 9, pp. 47-65.
- Böhm, H.J.; Han, W.; Eckschlager, A.** (2004): Multi-inclusion unit cell studies of reinforcement stresses and particle failure in discontinuously reinforced ductile matrix composites. *CMES: Computer Modeling in Engineering & Sciences*, vol. 5, no. 1, pp. 5-20.
- Bonfoh, N.; Lipinski, P.** (2007): Ductile damage micromodeling by particles' debonding in metal matrix composites. *International Journal of Mechanical Sciences*, vol. 49, pp. 151-160.
- Brown, L.M.; Embury, J.D.** (1973): The initiation and growth of voids at second phase particles. In: *Proceedings of 3rd International Conference on Strength of Metals and Alloys*, London, pp. 164-169.
- Chawla, N.; Chawla, K.K.** (2006): Microstructure-based modeling of the deformation behavior of particle reinforced metal matrix composites. *Journal of Materials Science*, vol. 41, pp. 913-925.
- Chen, J.K.; Huang, Z.P.; Mai, Y.W.** (2003): Constitutive relation of particulate-reinforced viscoelastic composite materials with debonded microvoids. *Acta Materialia*, vol. 51, pp. 3375-3384.

Dong, M.; Schmauder, S. (1996): Modeling of metal matrix composites by a self-consistent embedded cell model. *Acta Materialia*, vol. 44, pp. 2465-2478.

Drabek, T; Böhm, H.J. (2005): Damage models for studying ductile matrix failure in composites. *Composite Science and Technology*, vol. 32, pp. 329-336.

Eshelby, J.D. (1957): The determination of the elastic field of an ellipsoidal inclusion and related problems. *Proceedings of the Royal Society London A*, vol. 241, pp. 376-396.

Evans, R.D. (1999): *Damage evolution and micromechanisms in a small-particle metal-matrix composite*. Ph.D. Dissertation, Queen's University.

Ghosh, S.; Moorthy, S. (1998): Particle fracture simulation in non-uniform microstructures of metal-matrix composites. *Acta Materialia*, vol. 46, pp. 965-982.

Gurson, A.L. (1977): Continuum theory of ductile rupture by void nucleation and growth, Part I-Yield criteria and flow rules for porous ductile media. *Journal of Engineering Materials and Technology*, vol. 99, pp. 2-15.

Han, W.; Eckschlager, A.; Böhm, H.J. (2001): The effects of three-dimensional multi-particle arrangements on the mechanical behavior and damage initiation of particle-reinforced MMCs. *Composites Science and Technology*, vol. 61, pp. 1581-1590.

Haasemann, G.; Kástner, M.; Ulbricht, V. (2009): A new modelling approach based on Binary Model and X-FEM to investigate the mechanical behaviour of textile reinforced composites. *CMES: Computer Modeling in Engineering & Sciences*, vol. 42, no. 1, pp. 35-58.

Hazanov, S.; Huet, C. (1994): Order relationships for boundary condition effects in heterogeneous bodies smaller than the representative volume. *Journal of the Mechanics and Physics of Solids*, vol. 41, pp. 1995-2011.

Huber, G.; Brechet, Y.; Pardoën, T. (2005): Predictive model for void nucleation and void growth controlled ductility in quasi-eutectic cast aluminium alloys. *Acta Materialia*, vol. 53, pp. 2739-2749.

Hussain, A.K.; Adams, D.F. (2004): Analytical evaluation of the two-rail shear test method for composite materials. *Composites Science and Technology*, vol. 64, pp. 221-238.

Ibrahim, I.A.; Mohamed, F.A.; Lavernia, E.J. (1991): Particulate reinforced metal-matrix composites-a review. *Journal of Materials Science*, vol. 26, pp. 1137-1156.

Inem, B.; Pollard, G. (1993): Interface structure and fractography of a magnesium-alloy, metal-matrix composite reinforced with SiC particles. *Journal of Materials Science*, vol. 28, pp. 4427-4434.

Ju, J.W.; Chen, T.M. (1994): Micromechanics and effective elastoplastic behavior of two-phase metal matrix composites. *ASME Journal of Engineering Material and Technology*, vol. 116, pp. 310-318.

Ju, J.W.; Lee, H.K. (2000): A micromechanical damage model for effective elastoplastic behavior of ductile matrix composites considering evolutionary complete particle debonding. *Computer Methods in Applied Mechanics and Engineering*, vol. 183, pp. 201-222.

Ju, J.W.; Lee, H.K. (2001): A micromechanical damage model for effective elastoplastic behavior of partially debonded ductile matrix composites. *International Journal of Solids and Structures*, vol. 38, nos. 36-37, pp. 6307-6332.

Ju, J.W.; Sun, L.Z. (2001): Effective elastoplastic behavior of metal matrix composites containing randomly located aligned spheroidal inhomogeneities. Part I: micromechanics-based formulation. *International Journal of Solids and Structures*, vol. 38, pp. 183-201.

Ju, J.W.; Tseng, K.H. (1996): Effective elastoplastic behavior of two-phase ductile matrix composites: a micromechanical framework. *International Journal of Solids and Structures*, vol. 33, pp. 4267-4291.

Kaw, A.K. (1997): *Mechanics of Composite Materials*, CRC-Press.

Khisaeva, Z.F.; Ostoja-Starzewski, M. (2006): On the size of RVE in finite elasticity of random composites. *Journal of Elasticity*, vol. 85, pp. 153-173.

Kim, B.R.; Lee, H.K. (2009): Elastic-damage modeling for particulated composites considering the cumulative damage. *International Journal of Damage Mechanics*, accepted.

Lee, H.K.; Simunovic, S. (2001): A damage constitutive model of progressive debonding in aligned discontinuous fiber composites. *International Journal of Solids and Structures*, vol. 38, pp. 875-895.

Lewis, C.A.; Withers, P.J. (1995): Weibull modeling of particle cracking in metal matrix composites. *Acta Metallurgica et Materialia*, vol. 43, pp. 3685-3699.

Li, S.G.; Wongsto, A. (2004): Unit cells for micromechanical analyses of particle-reinforced composites. *Mechanics of Materials*, vol. 36, pp. 543-572.

Liu, H.T.; Sun, L.Z.; Ju, J.W. (2004): An interfacial debonding model for particle-reinforced composites. *International Journal of Damage Mechanics*, vol. 13, no. 2, pp. 163-185.

Llorca, J.; González, C. (1998): Microstructural factors controlling the strength and ductility of particle reinforced metal-matrix composites. *Journal of the Mechanics and Physics of Solids*, vol. 46, pp. 1-28.

Llorca, J.; Needleman, A.; Suresh, S. (1991): An analysis of the effects of ma-

trix void growth on deformation and ductility in metal-ceramic composites. *Acta Metallurgica et Materials*, vol. 39, no. 10, pp. 1317-1335.

Markgraaff, J. (1996): Overview of new developments in composite materials for industrial and mining applications. *Journal of the South African Institute of Mining and Metallurgy*, pp. 55-65, March/April.

McCintock, F.A. (1986): A criterion for ductile fracture by the growth of holes. *Journal of Applied Mechanics*, vol. 35, pp. 363-371.

Minak, G.; Chimisso, F.E.G.; Costa Mattos, H.S. (2005): Cyclic plasticity and damage of a metal matrix composite by a gradient-enhanced CDM model. *Structural Integrity & Durability*, vol. 1, no. 3, pp. 193-202.

Papazian, J.M.; Adler, P.N. (1990): Tensile properties of short fiber-reinforced SiC/Al composites, Part I: effect of matrix precipitates. *Metallurgical Transactions*, vol. A21, pp. 401-410.

Pahr, D.H.; Böhm, H.J. (2008): Assessment of mixed uniform boundary conditions for predicting the mechanical behavior of elastic and inelastic discontinuously reinforced composites. *CMES: Computer Modeling in Engineering & Sciences*, vol. 34, no. 2, pp. 117-136.

Rajan, T.P.D.; Pillai, R.M.; Pai, B.C. (1998): Reinforcement coatings and interfaces in aluminium metal matrix composites. *Journal of Materials Science*, vol. 33, pp. 3491-3503.

Rice, J.R.; Tracey, D.M. (1969): On the ductile enlargement of voids in triaxial stress fields. *Journal of Mechanics and Physics of Solids*, vol. 17, pp. 201-217.

Takashima, S.; Nakagaki, M.; Miyazaki, N. (2007): An elastic-plastic constitutive equation taking account of particle size and its application to a homogenized finite element analysis of a composite material. *CMES: Computer Modeling in Engineering & Sciences*, vol. 20, no. 3, pp. 193-202.

Tohgo, K.; Weng, G.J. (1994): A progressive damage mechanics in particle-reinforced metal-matrix composites under high triaxial tension. *Journal of Engineering Materials and Technology*, vol. 116, pp. 414-420.

Tvergaard, V. (1996): Effect of void size difference on growth and cavitation instabilities. *Journal of the Mechanics and Physics of Solids*, vol. 44, pp. 1237-1253.

Wallin, K.; Saario, T.; Törrönen, K. (1987): Fracture of brittle particles in a ductile matrix. *International Journal of Fracture*, vol. 32, pp. 201-209.

Wang, H.; Yao, Z. (2005): A new fast multiple boundary element method for large scale analysis of mechanical properties in 3D particle-reinforced composites. *CMES: Computer Modeling in Engineering & Sciences*, vol. 7, no. 1, pp. 85-95.

Zhao, Y.H.; Weng, G.J. (1995): A theory of inclusion debonding and its influence

on the stress-strain relations of a ductile matrix. *International Journal of Damage Mechanics*, vol. 4, pp. 196-211.

Zong, B.Y.; Zhang, F.; Wang, G.; Zuo, L. (2007): Strengthening mechanism of load sharing of particulate reinforcements in a metal matrix composites. *Journal of Materials Science*, vol. 42, pp. 4218-4226.

Appendix I Recapitulation of cumulative damage model [Kim and Lee (2009)]

The cumulative damage model proposed by Kim and Lee (2009) is recapitulated for completeness of the proposed incremental damage model. In phenomenological aspect of gradually evolutionary damage, the subsequent damage states are affected by the current and previous damage states and these damage states are accumulated as illustrated in Fig. 11. Following Kim and Lee (2009), the cumulative damage model for the gradually incremental damage can be expressed as [Kim and Lee (2009)]

$$F_1[(\bar{\sigma}_p)_1] = 1 - \exp \left\{ - \left[\frac{(\bar{\sigma}_p)_1}{(S_0)_1} \right]^M \right\} \quad (16)$$

$$F_n[(\bar{\sigma}_p)_n] = 1 - \exp \left\{ - \left[\frac{[(\bar{\sigma}_p)_n - (\bar{\sigma}_p)_{n-1}] + (\sigma_{eq})_{n-1}}{(S_0)_n} \right]^M \right\} \quad (n = 2, \dots, N) \quad (17)$$

with

$$(\sigma_{eq})_{n-1} = [(\bar{\sigma}_p)_{n-1} - (\bar{\sigma}_p)_{n-2}] \left[\frac{(S_0)_n}{(S_0)_{n-1}} \right] + (\sigma_{eq})_{n-2} \quad (18)$$

where $(\sigma_{eq})_{n-1}$ is the equivalent stress for the n^{th} damage step. Considering the proposed damage model, the current volume fraction of each phase (completely debonded particles, partially debonded particles, and perfectly bonded particles) for the proposed incremental damage model can be expressed as

$$\phi_3 = \phi \left[1 - \exp \left\{ - \left[\frac{(\bar{\sigma}_p)_1}{(S_0)_1} \right]^M \right\} \right] \cdot \left[1 - \exp \left\{ - \left[\frac{[(\bar{\sigma}_p)_2 - (\bar{\sigma}_p)_1] + (\sigma_{eq})_1}{(S_0)_2} \right]^M \right\} \right] \quad (19)$$

$$\phi_2 = \phi \left[1 - \exp \left\{ - \left[\frac{(\bar{\sigma}_p)_1}{(S_0)_1} \right]^M \right\} \right] - \phi_3 \quad (20)$$

$$\phi_1 = \phi - \phi_2 - \phi_3 \quad (21)$$

with

$$(\sigma_{eq})_1 = (\bar{\sigma}_p)_1 \left[\frac{(S_0)_2}{(S_0)_1} \right] \tag{22}$$

where ϕ is the original particle volume fraction, ϕ_r is the r -phase volume fraction, and $(S_0)_1, (S_0)_2$, and M are the Weibull parameters. In addition, $\bar{\sigma}_p$ is the (averaged) internal stress and $(\cdot)_r$ denotes the r -phase. Details of the cumulative damage model can be found in Kim and Lee (2009).

Appendix II Parameters T_1, \dots, T_6 in Eq. (10)

The parameters T_1, \dots, T_6 in Eq. (10) are the components of the fourth-rank tensor $\tilde{F}_{ijkl}(T_1, \dots, T_6)$ and take the form:

$$T_1 = \frac{\phi_2}{35} \{ 840\mu_0(\xi_2 + 5\xi_4) + 2880\mu_0^2(7\xi_1^2 + 56\xi_1\xi_2 + 28\xi_2^2 + 22\xi_2\xi_4 + 42\xi_1\xi_6 + 26\xi_2\xi_6 + 30\xi_4\xi_6) - 13440\mu_0^2[(3\xi_1^2 + 24\xi_1\xi_2 + 12\xi_2^2 + 24\xi_2\xi_4 + 18\xi_2\xi_5 + 18\xi_1\xi_6 + 26\xi_2\xi_6 + 10\xi_4\xi_6) + 2\nu_0(-3\xi_2\xi_4 + 9\xi_2\xi_5 + 4\xi_2\xi_6 + 2\xi_4\xi_6)] + \frac{5600}{3}\mu_0^2[5(5\xi_1^2 + 40\xi_1\xi_2 + 32\xi_2^2 + 6\xi_1\xi_3 + 24\xi_2\xi_3 + 9\xi_3^2 + 40\xi_2\xi_4 + 48\xi_2\xi_5 + 24\xi_1\xi_6 + 44\xi_2\xi_6) + 10\nu_0(-\xi_1^2 8\xi_1\xi_2 + 8\xi_2^2 + 6\xi_1\xi_3 + 24\xi_2\xi_3 + 9\xi_3^2 - 8\xi_2\xi_4 + 12\xi_2\xi_5 - 12\xi_1\xi_6 + 8\xi_2\xi_6 + 12\xi_4\xi_6) + \nu_0^2(19\xi_1^2 + 152\xi_1\xi_2 + 136\xi_2^2 + 30\xi_1\xi_3 + 120\xi_2\xi_3 + 45\xi_3^2 - 28\xi_2\xi_4 - 120\xi_2\xi_5 + 84\xi_1\xi_6 - 104\xi_2\xi_6 - 60\xi_4\xi_6)] \} \tag{23}$$

$$T_2 = \frac{\phi_2}{35} \{ 1260\mu_0\xi_2 + 1440\mu_0^2\xi_2(153\xi_2 + 194\xi_6) + 6720\mu_0^2\xi_2[-(67\xi_2 + 6\xi_6) + 2\nu_0(\xi_2 - 54\xi_6)] + 5600\mu_0^2\xi_2[40(2\xi_2 + \xi_6) - 10\nu_0(9\xi_2 + 10\xi_6) + \nu_0^2(61\xi_2 + 178\xi_6)] \} \tag{24}$$

$$T_3 = \frac{\phi_2}{35} \{ -4200\mu_0\xi_2 + 2880\mu_0^2(7\xi_1\xi_4 + 17\xi_2\xi_4 - 7\xi_1\xi_6 - 13\xi_2\xi_6 + 6\xi_4\xi_6) + 13440\mu_0^2[(-3\xi_1\xi_4 + 9\xi_2\xi_5 + 3\xi_1\xi_6 - 7\xi_2\xi_6 - 4\xi_4\xi_6) + \nu_0(-3\xi_2\xi_4 + 9\xi_2\xi_5 + 32\xi_2\xi_6 + 2\xi_4\xi_6)] + \frac{5600}{3}\mu_0^2[5(5\xi_1\xi_4 + 3\xi_3\xi_4 + 3\xi_1\xi_5 - 12\xi_2\xi_5 + 9\xi_3\xi_5 - 2\xi_1\xi_6 + 6\xi_2\xi_6 + 6\xi_3\xi_6 + 12\xi_4\xi_6) + 10\nu_0(-\xi_1\xi_4 + 3\xi_3\xi_4 + 3\xi_1\xi_5 + 6\xi_2\xi_5 + 9\xi_3\xi_5 + 4\xi_1\xi_6 + 6\xi_3\xi_6 - 12\xi_4\xi_6) + \nu_0^2(19\xi_1\xi_4 + 90\xi_2\xi_4 + 15\xi_3\xi_4 + 15\xi_1\xi_5 + 120\xi_2\xi_5 + 45\xi_3\xi_5 - 4\xi_1\xi_6 - 48\xi_2\xi_6 + 30\xi_3\xi_6 + 72\xi_4\xi_6)] \} \tag{25}$$

$$T_4 = \frac{\phi_2}{35} \{ -4200\mu_0\xi_4 + 2880\mu_0^2(7\xi_1\xi_4 + 17\xi_2\xi_4 - 7\xi_1\xi_6 - 13\xi_2\xi_6 + 6\xi_4\xi_6) + 13440\mu_0^2[(-3\xi_1\xi_4 + 9\xi_2\xi_5 + 3\xi_1\xi_6 - 7\xi_2\xi_6 - 4\xi_4\xi_6) + \nu_0(-3\xi_2\xi_4 + 9\xi_2\xi_5 + 32\xi_2\xi_6 + 2\xi_4\xi_6)] + \frac{5600}{3}\mu_0^2[5(5\xi_1\xi_4 + 3\xi_3\xi_4 + 3\xi_1\xi_5 - 12\xi_2\xi_5 + 9\xi_3\xi_5 - 2\xi_1\xi_6 + 6\xi_2\xi_6 + 6\xi_3\xi_6 + 12\xi_4\xi_6) + 10\nu_0(-\xi_1\xi_4 + 3\xi_3\xi_4 + 3\xi_1\xi_5 + 6\xi_2\xi_5 + 9\xi_3\xi_5 + 4\xi_1\xi_6 + 6\xi_3\xi_6 - 12\xi_4\xi_6) + \nu_0^2(19\xi_1\xi_4 + 90\xi_2\xi_4 + 15\xi_3\xi_4 + 15\xi_1\xi_5 + 120\xi_2\xi_5 + 45\xi_3\xi_5 - 4\xi_1\xi_6 - 48\xi_2\xi_6 + 30\xi_3\xi_6 + 72\xi_4\xi_6)] \} \quad (26)$$

$$T_5 = -\frac{1}{3} + \frac{\phi_2}{35} \{ -20160\mu_0^2(\xi_4^2 - 2\xi_4\xi_6 + 2\xi_6^2) + \frac{5600}{3}\mu_0^2[5(5\xi_4^2 + 6\xi_4\xi_5 + 9\xi_5^2 - 4\xi_4\xi_6 + 12\xi_5\xi_6 - 4\xi_6^2) + 10\nu_0(-\xi_4^2 + 6\xi_4\xi_5 + 9\xi_5^2 + 8\xi_4\xi_6 + 12\xi_5\xi_6 + 8\xi_6^2) + \nu_0^2(19\xi_4^2 + 30\xi_4\xi_5 + 45\xi_5^2 - 8\xi_4\xi_6 + 60\xi_5\xi_6 - 8\xi_6^2)] \} + \frac{200}{3}(1 - 2\nu_0)^2 \left[\frac{\phi_1}{(3\alpha_1 + 2\beta_1)^2} + \frac{\phi_3}{(3\alpha_3 + 2\beta_3)^2} \right] - 2(23 - 50\nu_0 + 35\nu_0^2) \left[\frac{\phi_1}{\beta_1^2} + \frac{\phi_3}{3\beta_3^2} \right] \quad (27)$$

$$T_6 = \frac{1}{2} + \frac{\phi_2}{35} \{ -2100\mu_0\xi_6 + 99360\mu_0^2\xi_6 + 6720\mu_0^2\xi_6^2(-31 + 2\nu_0) + 5600\mu_0^2\xi_6^2(40 - 50\nu_0 + 33\nu_0^2) \} + 2(23 - 50\nu_0 + 35\nu_0^2) \left[\frac{\phi_1}{\beta_1^2} + \frac{\phi_3}{\beta_3^2} \right] \quad (28)$$

with

$$\alpha_1 = 2(5\nu_0 - 1) + 10(1 - \nu_0) \left(\frac{\kappa_0}{\kappa_1 - \kappa_0} - \frac{\mu_0}{\mu_1 - \mu_0} \right), \quad (29)$$

$$\beta_1 = 2(4 - 5\nu_0) + 15(1 - \nu_0) \frac{\mu_0}{\mu_1 - \mu_0}$$

$$\alpha_3 = 2(5\nu_0 - 1), \quad \beta_3 = 5\nu_0 - 7 \quad (30)$$

where ν_0 denotes the Poisson's ratio in the matrix, and the parameters ξ_1, \dots, ξ_6 are given by [Ju and Lee (2001)]

$$\xi_1 = \frac{-\eta_2\eta_3\eta_4 + (\eta_1\eta_2 + 4\eta_2^2)\eta_5 + (2\eta_1\eta_2 + 8\eta_2^2 + 4\eta_2\eta_3 + 4\eta_2\eta_4 + 3\eta_3\eta_4 - 3\eta_1\eta_5 - 2\eta_1\eta_6)\eta_6}{8\eta_6(\eta_2 + \eta_6)[- \eta_3\eta_4 + (\eta_1 + 4\eta_2)\eta_5 + (\eta_1 + 4\eta_2 + \eta_3 + \eta_4 + 3\eta_5 + 2\eta_6)\eta_6]\mu_0} \quad (31)$$

$$\xi_2 = \frac{-\eta_2}{8\eta_6(\eta_2 + \eta_6)\mu_0} \tag{32}$$

$$\xi_3 = \frac{-\eta_3\eta_4 + (\eta_1 + 4\eta_2)\eta_5 - 2\eta_3\eta_6}{8\eta_6[-\eta_3\eta_4 + (\eta_1 + 4\eta_2)\eta_5 + (\eta_1 + 4\eta_2 + \eta_3 + \eta_4 + 3\eta_5 + 2\eta_6)\eta_6]\mu_0} \tag{33}$$

$$\xi_4 = \frac{[-9\eta_3\eta_4 + 9(\eta_1 + 4\eta_2)\eta_5 + 6(\eta_1 + 4\eta_2)\eta_6]\kappa_0 - 4(\eta_1 + 4\eta_2 + 3\eta_4)\eta_6\mu_0}{72\eta_6[-\eta_3\eta_4 + (\eta_1 + 4\eta_2)\eta_5 + (\eta_1 + 4\eta_2 + \eta_3 + \eta_4 + 3\eta_5 + 2\eta_6)\eta_6]\kappa_0\mu_0} \tag{34}$$

$$\xi_5 = \frac{[9\eta_3\eta_4 - 9(\eta_1 + 4\eta_2)\eta_5 - 6(\eta_1 + 4\eta_2 + \eta_4 + 3\eta_5 + 2\eta_6)\eta_6]\kappa_0 + 4(\eta_1 + 4\eta_2 + \eta_4 + 2\eta_6)\eta_6\mu_0}{72\eta_6[-\eta_3\eta_4 + (\eta_1 + 4\eta_2)\eta_5 + (\eta_1 + 4\eta_2 + \eta_3 + \eta_4 + 3\eta_5 + 2\eta_6)\eta_6]\kappa_0\mu_0} \tag{35}$$

$$\xi_6 = \frac{1}{8\eta_6\mu_0} \tag{36}$$

in which

$$\eta_1 = -60(1 - \nu_0) \frac{\mu_1}{\mu_0 - \mu_1} \cdot \frac{3\kappa_0\kappa_1(\mu_0 - \mu_1) + \mu_0\mu_1(\kappa_0 - \kappa_1)}{3\kappa_0\kappa_1(\mu_0 - \mu_1) + 4\mu_0\mu_1(\kappa_0 - \kappa_1)} \tag{37}$$

$$\eta_2 = 15(1 - \nu_0) \frac{\mu_1}{\mu_0 - \mu_1} \tag{38}$$

$$\eta_3 = 60(1 - \nu_0) \frac{\mu_0\mu_1}{\mu_0 - \mu_1} \cdot \frac{\kappa_1\mu_0 - \kappa_0\mu_1}{3\kappa_0\kappa_1(\mu_0 - \mu_1) + 4\mu_0\mu_1(\kappa_0 - \kappa_1)} \tag{39}$$

$$\eta_4 = 30(1 - \nu_0) \frac{\mu_1}{\mu_0 - \mu_1} \cdot \frac{3\kappa_0\kappa_1(\mu_0 - \mu_1) - 2\mu_0\mu_1(\kappa_0 - \kappa_1)}{3\kappa_0\kappa_1(\mu_0 - \mu_1) + 4\mu_0\mu_1(\kappa_0 - \kappa_1)} \tag{40}$$

$$\eta_5 = 2(5\nu_0 - 1) - 60(1 - \nu_0) \frac{\mu_0\mu_1}{\mu_0 - \mu_1} \cdot \frac{\kappa_1\mu_0 - \kappa_0\mu_1}{3\kappa_0\kappa_1(\mu_0 - \mu_1) + 4\mu_0\mu_1(\kappa_0 - \kappa_1)} \tag{41}$$

$$\eta_6 = 2(4 - 5\nu_0) - 15(1 - \nu_0) \frac{\mu_0}{\mu_0 - \mu_1} \tag{42}$$

Appendix III Parameters P_1, \dots, P_6 in Eq. (11)

The parameters P_1, \dots, P_6 in Eq. (11) are the components of the fourth-rank tensor $\tilde{F}_{ijkl}(P_1, \dots, P_6)$ and take the form:

$$P_6 = \frac{1}{4\Gamma_6}, \quad P_2 = -\frac{\Gamma_2}{4\Gamma_6(\Gamma_2 + \Gamma_6)} \quad (43)$$

$$\begin{Bmatrix} P_1 \\ P_4 \end{Bmatrix} = D^{-1} \begin{Bmatrix} -2P_6\Gamma_1 - 4P_2(\Gamma_1 + 2\Gamma_2 + \Gamma_3) \\ -2P_6\Gamma_4 - 4P_2(\Gamma_4 + \Gamma_5) \end{Bmatrix}, \quad \begin{Bmatrix} P_3 \\ P_5 \end{Bmatrix} = D^{-1} \begin{Bmatrix} -2P_6\Gamma_3 \\ -2P_6\Gamma_5 \end{Bmatrix} \quad (44)$$

with

$$D \equiv \begin{bmatrix} \Gamma_1 + 4\Gamma_2 + \Gamma_3 + 2\Gamma_6 & \Gamma_1 + 4\Gamma_2 + 3\Gamma_3 \\ \Gamma_4 + \Gamma_5 & \Gamma_4 + 3\Gamma_5 + 2\Gamma_6 \end{bmatrix} \quad (45)$$

where the coefficients $\Gamma_1, \dots, \Gamma_6$ read

$$\Gamma_1 = \frac{\phi_1(-7 + 5\nu_0)[- \eta_2\eta_3\eta_4 + (\eta_1\eta_2 + 4\eta_2^2)\eta_5 + (2\eta_1\eta_2 + 8\eta_2^2 + 4\eta_2\eta_3 + 4\eta_2\eta_4 + 3\eta_3\eta_4 - 3\eta_1\eta_5 + 2\eta_1\eta_6)\eta_6]}{2\eta_6(\eta_2 + \eta_6)[- \eta_3\eta_4 + (\eta_1 + 4\eta_2)\eta_5 + (\eta_1 + 4\eta_2 + \eta_3 + 3\eta_5 + 2\eta_6)\eta_6]} \quad (46)$$

$$\Gamma_2 = \frac{\phi_2\eta_2(-7 + 5\nu_0)}{2\eta_6(\eta_2 + \eta_6)} \quad (47)$$

$$\Gamma_3 = \frac{\phi_2[(7 - 5\nu_0)\{\eta_3\eta_4 - (\eta_1 + 4\eta_2)\eta_5\} + 2(1 - 5\nu_0)(\eta_1 + 4\eta_2)\eta_6 + 20(1 - 2\nu_0)\eta_3\eta_6]}{2\eta_6[- \eta_3\eta_4 + (\eta_1 + 4\eta_2)\eta_5 + (\eta_1 + 4\eta_2 + \eta_3 + 3\eta_5 + 2\eta_6)\eta_6]} \quad (48)$$

$$\Gamma_4 = \frac{\phi_2(-7 + 5\nu_0)[- \eta_3\eta_4 + (\eta_1 + 4\eta_2)\eta_5] - 2\eta_4\eta_6}{2\eta_6[- \eta_3\eta_4 + (\eta_1 + 4\eta_2)\eta_5 + (\eta_1 + 4\eta_2 + \eta_3 + 3\eta_5 + 2\eta_6)\eta_6]} \quad (49)$$

$$\Gamma_5 = \frac{[(-7 + 5\nu_0)\alpha_1 + 2(1 - 5\nu_0)\beta_1]\phi_1}{\beta_1(3\alpha_1 + 2\beta_1)} + \frac{\phi_2(-7 + 5\nu_0)[- \eta_3\eta_4 + (\eta_1 + 4\eta_2)\eta_5] - 2\eta_4\eta_6}{2\eta_6[- \eta_3\eta_4 + (\eta_1 + 4\eta_2)\eta_5 + (\eta_1 + 4\eta_2 + \eta_3 + 3\eta_5 + 2\eta_6)\eta_6]} + \frac{[(-7 + 5\nu_0)\alpha_3 + 2(1 - 5\nu_0)\beta_3]\phi_3}{\beta_3(3\alpha_3 + 2\beta_3)} \quad (50)$$

$$\Gamma_6 = \frac{1}{2} + (7 - 5\nu_0) \cdot \left[\frac{\phi_1}{2\beta_1} - \frac{\phi_2}{2\eta_6} + \frac{\phi_3}{2\beta_3} \right] \quad (51)$$

